Electrochimica Acta, Vol. 32, No. 5, pp. 815–821, 1987.
Printed in Great Britain.

0013–4686/87 $3.00 + 0.00

THE ELECTROCHEMICAL REDUCTION OF Sn(II) AT THE DROPPING MERCURY ELECTRODE FROM AQUEOUS 1 M SULFURIC ACID AND FROM 0.3 M PHENOLSULPHONIC ACID AND ITS INHIBITION BY ENSA-6

C. J. VAN VELZEN, M. SLUYTERS-REHBACH and J. H. SLUYTERS

Van't Hoff laboratory, State University Utrecht, Padualaan 8, 3584 CH Utrecht, The Netherlands

(*Received* 27 *August* 1986)

Abstract—By means of the demodulation technique for the first time the high reduction rate constant of the Sn(II) ion in sulfuric acid is obtained. From the value of the operational transfer coefficient it follows that a following, potential independent "chemical" step is rate determining. On the addition of an inhibitor at positive potentials the transfer of the first electron can be made slow because this process is inhibited much more strongly than the following chemical step. At high concentration of the inhibitor the first electron transfer is rate determining at all potentials. In phenolsulphonic acid as the base electrolyte it appears that an intermediate chemical step is rate controlling together with the following chemical step. The intermediate step could be made rate determining by adding a little of the inhibitor. With a high concentration of the inhibitor the first electron transfer becomes rate controlling again. Also the reduction of Sn(II) from a practical plating bath is discussed.

INTRODUCTION

An important application of tin is its use in steel plating More than 99% of all tin plate is performed by electrodeposition[1]. The electrochemical properties of tin have not been studied extensively. A review on the electrochemical research done before 1977 has been given by Stirrup and Hampson[2]. Kinetic parameters on the reduction of Sn(II) ions have been obtained only in the presence of an inhibitor[3], evidently because without an inhibitor the value of the reduction rate constant exceeds the upper limit accessible with the usual techniques. Another difficulty is the instability of the Sn(II) ions in the presence of oxygen, by which it can easily be oxidized[3].

The purpose of the present work is to investigate the influence of an inhibitor on the kinetics and the mechanism of the reduction of Sn(II) ions. To that end this reaction first has to be studied in the absence of the inhibitor. This seems to be feasible nowadays with the demodulation technique that recently became available[4].

When the reduction rate is lowered by the presence of the inhibitor the impedance technique developed in our laboratory[5, 6] can be applied.

In our first attempts hexanol was selected as a model inhibitor. However, the impedance of the dropping mercury electrode in contact with solutions of the supporting electrolyte and hexanol did not correspond to the simple series connection of the ohmic resistance and a double layer capacitance. Both the resistive component and the (apparent) capacitance showed a very large frequency dispersion, which would complicate the analysis of the Sn(II) reduction too much. Evidently the adsorption behaviour of the alcohol is quite complex.

The inhibitor ENSA-6 (naphthalene sulphonic acid, ethoxylated with a chain of mainly six ethoxy-groups) employed in a practical tin plating electrolyte as a brightener, did not show this complicating effect. The influence of this inhibitor on the electrode reaction was therefore investigated by means of impedance and *dc* polarographic experiments, with sulfuric acid as the base electrolyte.

Because the practical plating bath contains phenolsulphonic acid as an antioxidant, instead of sulfuric acid, the reduction of Sn(II) has also been studied in that base electrolyte.

The ultimate purpose of this study is better to understand the kinetics and mechanism of the plating process on steel, where also nucleation and growth rates contribute to the overall process. This work, which is performed at the dropping mercury electrode, will not be complicated by the latter processes, giving a better chance to understand the reduction process *per se*.

EXPERIMENTAL

All measurements were performed with a three electrode cell, thermostated at 25°C. The working electrode was a dropping mercury electrode with a drawn-out capillary. All potentials are reported *vs* saturated calomel electrode (*sce*).

The *dc* polarographic and impedance measurements were performed with the automatic network analyzer system[6] described earlier. The demodulation polarograms were obtained with the instrument developed in this laboratory[4]. All measurements were made at exactly 4 s after drop birth.

The solutions were prepared from concentrated sulfuric acid and stannous sulfate of analytical grade and of phenolsulphonic acid of technical grade. The inhibitor ENSA-6 was supplied by the steel company

Hoogovens Groep, IJmuiden, The Netherlands. All these chemicals were used without further purification.

The electrolyte solutions were thoroughly deaerated by purging very pure nitrogen before the stannous sulfate was added.

THEORY

From the experimental results to be described in the next section it will become evident that the reduction of Sn(II) ions does not always proceed according to simple Butler–Volmer behaviour. This conclusion has to be drawn because of the nonlinear potential dependence of the logarithm of the overall reduction rate constant k_f, or, to say it otherwise, because of the potential dependence of the operational transfer coefficient

$$\alpha = -\frac{RT}{nF}\frac{\mathrm{d}\ln k_f}{\mathrm{d}E} = -\frac{\mathrm{d}\ln k_f}{\mathrm{d}\varphi}. \tag{1}$$

In order to keep the discussion general, we for the time being suppose the mechanism of the overall reaction

$$\mathrm{Sn(II)} + 2e \Leftrightarrow \mathrm{Sn(Hg)}$$

to consist of five steps, which is the maximal conceivable number:

C_1 preceeding chemical step $\mathrm{Sn(II)} \Leftrightarrow \mathrm{Sn(II)^*}$

E_1 first electron transfer $\mathrm{Sn(II)^*} + e \Leftrightarrow \mathrm{Sn(I)}$

C_2 intermediate chemical step $\mathrm{Sn(I)} \Leftrightarrow \mathrm{Sn(I)^*}$

E_2 second electron transfer $\mathrm{Sn(I)^*} + e \Leftrightarrow \mathrm{Sn^*}$

C_3 following chemical step $\mathrm{Sn^*} \Leftrightarrow \mathrm{Sn(Hg)}$.

As we have shown earlier[7–9], assuming stationary state behaviour and the absence of the diffusion of intermediates, for this sequence of steps the potential dependence of the reduction rate constant k_f of the overall process will be given by

$$1/k_f = \frac{1}{k_{c,1}} + \frac{\exp(1/2\,\alpha_1\varphi)}{k_{s,1}} + \frac{\exp(1/2\,\varphi)}{k_{c,2}} + \frac{\exp[1/2(1+\alpha_2)\varphi]}{k_{s,2}} + \frac{\exp(\varphi)}{k_{c,3}}, \tag{2}$$

with $\varphi = (nF/RT)(E - E^\circ)$. In this equation k_{c1}, k_{c2} and k_{c3} are the rate constants of the chemical steps, k_{s1} and k_{s2} are the standard rate constants, at $E = E^\circ$, the two one-electron transfers, α_1 and α_2 are their appurtenant transfer coefficients.

In equation (2) all terms may contribute within the experimentally accessible potential region; those steps that are absent or that do not show up, formally can be given a very large rate constant $k_{c,i}$ or $k_{s,i}$. If one rate constant is low the step it describes will be rate determining. Evidently more than one step can be rate controlling at the same time and also the relative preponderance of the steps in equation (2) will be different at different potentials.

It will be clear that the value of k_f should be obtained with a high accuracy and in a potential range as wide as possible in order to be able to detect the possible presence of a step *via* a computer fit of the experimental $k_f(\varphi)$ to equation (2).

The impedance measurements are usually performed at varied frequency (between 80 and 5000 Hz) and at varied potential within the accessible faradaic region. From the frequency dependence at each potential the charge transfer resistance R_{ct} is obtained by the usual analysis according to the Randles' circuit, the validity of which is confirmed by internal checks. If the system is *dc* reversible the value of k_f can be directly derived from[9]

$$R_{ct,\mathrm{rev}}^{-1} = \frac{n^2F^2}{RT}\frac{k_f C_O^*}{1 + (D_R/D_O)^{1/2}\exp(-\varphi)}. \tag{3}$$

If the system is non-*dc* reversible, R_{ct} is a function of both k_f and α. According to the diffusion layer model

$$R_{ct}^{-1} = \frac{n^2F^2}{RT}k_f C_O^*\frac{\alpha(a_O/k_f) + (a_O/a_R)\exp(\varphi)}{a_O/k_f + (a_O/a_R)\exp(\varphi) + 1}. \tag{4}$$

For the *dme* the most appropriate expression for a_O and a_R is[10]

$$a_{O,R} = \left(\frac{7D_i}{3\pi t}\right)^{1/2}\left(1 \pm 1.03\frac{D_i}{r_0}\right), \tag{5}$$

the plus sign pertaining to O, the minus sign to R.

In this work the values of k_f as a function of potential were obtained by describing $\ln k_f$ as a power series of φ, and $\alpha = -\mathrm{d}\ln k_f/\mathrm{d}\varphi$ as the derivative of this series. After substitution into equation (4) the coefficients of the series were derived from the best fit to R_{ct}^{-1}.

In the demodulation method, a current density of the type $\Delta j = j_A \sin(\omega_H t)\cos(\omega_L t)$ is forced through the cell, and the demodulation voltage response,

$$\Delta E = I_{LF}\cos(2\omega_L t) + Q_{LF}\sin 2\omega_L t$$

is measured[4]. The condition $\omega_H \gg \omega_L$ together with technical restrictions at high frequencies bounds the useful high frequency range within about 100 kHz–1 MHz. Therefore the demodulation voltammograms, I_{LF} and Q_{LF} as a function of *dc* potential, are recorded at fixed ω_H. The in-phase component I_{LF} and the quadrature component Q_{LF} are dependent on both first and second order faradaic and double-layer parameters (see Refs [4] and [8]). The essential parameters are

$$\lambda = k_f[D_O^{-1/2} + D_R^{-1/2}\exp(\varphi)], \tag{6}$$

$$S_F^* = \frac{\frac{1}{2}D_O^{1/2}\exp(\varphi) - D_R^{1/2}}{\frac{1}{2}D_O^{1/2}\exp(\varphi) + D_R^{1/2}}\frac{(p_H+2) + (\alpha - 1/2)(p_H^2 + p_H)}{(p_H+1)^2 + (a_H+1)^2} \tag{7}$$

with $p_H = (2\omega_H)^{1/2}/\lambda$ and $a_H = p_H/(R_{ct}\omega_H C_d)$. Equation (7) holds in the case of a linear rate equation and *dc* reversible charge transfer. So, here also in the *dc* reversible case the above-mentioned polynomial approach is required to obtain k_f and α as a function of E or φ. In addition the second order double-layer contribution has to be accounted for by calculating the parameter

$$[S_c] = -\frac{1}{2C_d}\frac{\mathrm{d}C_d}{\mathrm{d}E}\frac{j_A^2}{(2\omega_H C_d)^2}\frac{(p_H+1)^2+1}{(p_H+1)^2+(a_H+1)^2} \tag{8}$$

where C_d is the double-layer capacitance, measured with the impedance method. Its derivative with respect to E is calculated from a 12th degree polynomial fit to $C_d = f(E)$[8].

The $k_f(\varphi)$ data obtained following the above routes can be fitted to equation (2), delivering the values of the individual rate constants k_{c1}, k_{s1}, *etc.* All analyses were made on the assumption that $\alpha_1 = \alpha_2 = 0.5$. The effect of the inhibitor can then be described in terms of the relationship between rate constants and inhibitor concentration. Here a considerable complication arises because the inhibitor undoubtedly acts *via* its adsorption and therefore its effect should be interpreted *via* its surface excess, which will in general be both dependent on concentration, potential and, at a dropping mercury electrode, on time. This complication here will be dealt with only in part, the description at constant inhibitor concentration evidently leading to sensible results under the circumstances of these experiments.

RESULTS

Reduction from sulfuric acid solution without inhibitor

In this electrolyte the reduction of Sn(II) was found to be *ac* reversible. Consequently by means of the impedance technique only the diffusion coefficient and the half-wave potential could be obtained. They were found to be 6.0×10^{-6} cm^2 s^{-1} and -0.420 V *vs sce*, respectively.

The demodulation polarograms were obtained in 1 M H_2SO_4 with 1 mM $SnSO_4$ at two different combinations of ω_H and ω_L, *viz.* 175 kHz + 381 Hz and 100 kHz + 229 Hz, leading to results that were identical within experimental accuracy.

The components of the demodulation polarograms are reproduced in Fig. 1. The experimental results were processed as described in the preceeding section, leading to the conclusion that only the very last step was rate determining with $k_{c3} = 3.5 \pm 0.5$ cm s^{-1}. The solidity of this finding is evident from the quality of the fit in Fig. 1a and b and from the value of the operational transfer coefficient $\alpha = -(\mathrm{d} \ln k_f)/(\mathrm{d}\varphi) = 0.95 \pm 0.05$, that appeared to be constant in the useful potential region.

A mechanism comprising a dismutation step $2\,\mathrm{Sn(I)} \Leftrightarrow \mathrm{Sn} + \mathrm{Sn(II)}$ could not be reconciled with the experimental Fig. 1.

In accordance with literature the rate constant is very high. The high value of the operational cathodic transfer coefficient indicates that neither of the two electron transfers is rate controlling and that a following chemical step is rate determining. This step might be the dissolution of tin atoms into the mercury or possibly the formation of an intermetallic compound with mercury. Also a slow loss of a hydration shell around the tin atom could act as a step following the two much faster electron transfers.

Reduction from sulfuric acid solution in the presence of the inhibitor ENSA-6

Already quite low concentrations of the inhibitor ENSA-6 give a considerable lowering of the double layer capacitance which indicates its strong adsorption at the mercury–electrolyte interface (Fig. 2).

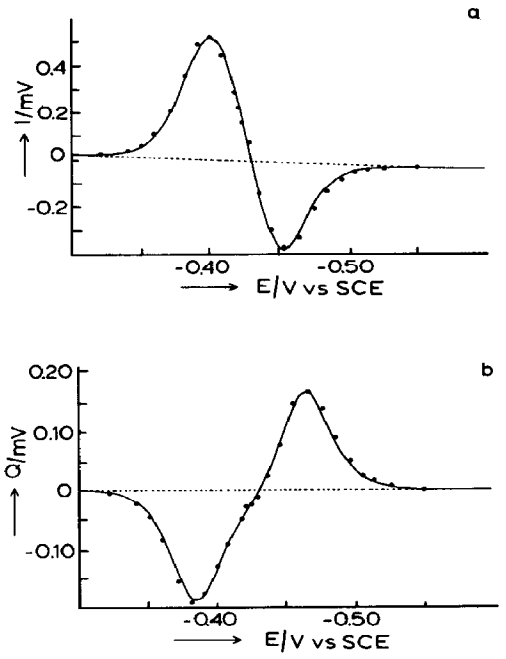

Fig. 1. Demodulation voltammograms of 1 mM $SnSO_4$ in 1 M H_2SO_4 solution: (a) in-phase component, (b) quadrature component. The low frequency is 230 Hz, the high frequency is 100 kHz. Experimental points are indicated by dots. The drawn curves are calculated with $k_f = 3.5 \exp(-1.00\varphi)$.

In spite of this a concentration of 7 ppm ENSA-6 is needed to slow down the Sn(II) reduction to such an extent that it can be studied with the impedance method. Fortunately also at high concentration, up to 2000 ppm, the frequency dependence of the interfacial admittance remains in accordance with the Randles–Ershler equivalent circuit. Consequently the analysis at all ENSA-6 concentrations could be performed as usual[5].

In Fig. 3 the experimental charge transfer resistance is reproduced as a function of electrode potential and at ENSA-6 concentrations between 7 and 50 ppm. From these plots the reduction rate constant as a function of potential was derived and it was found that in the presence of the inhibitor Butler–Volmer behaviour was not obeyed (Fig. 4). It was concluded that for the inhibited reduction the first electron transfer and the third chemical step together are rate determining. Evidently the first electron transfer E_1 is slowed down so much by the inhibitor that it shows up in the kinetics, despite that also the following reaction C_3 slows down dramatically. The deceleration of the first electron transfer could be followed down to very low values. In Table 1 both k_{s1} and k_{c3} are reported in the accessible concentration ranges of the inhibitor.

Reduction from phenolsulphonic acid solution and its inhibition by ENSA-6

The overall rate constant of the reduction of Sn(II) from aqueous 1 M phenolsulphonic acid solution is

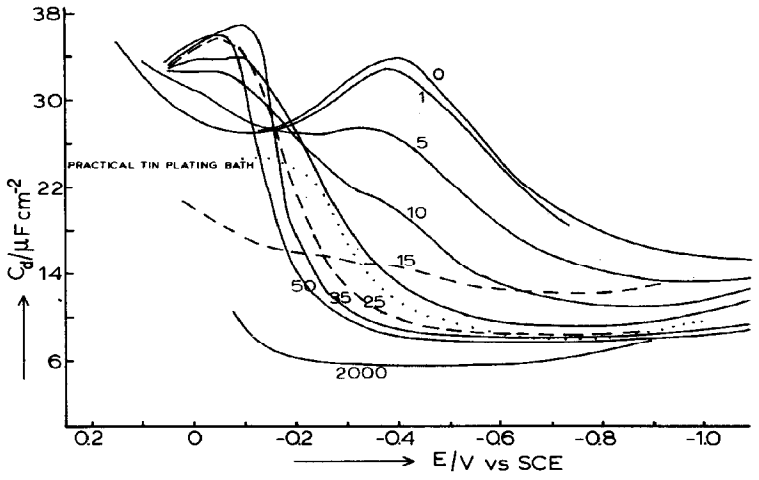

Fig. 2. Double-layer capacitances of the *dme* in contact with 1 M H_2SO_4 solutions containing ENSA-6. Concentrations of the latter are indicated in ppm.

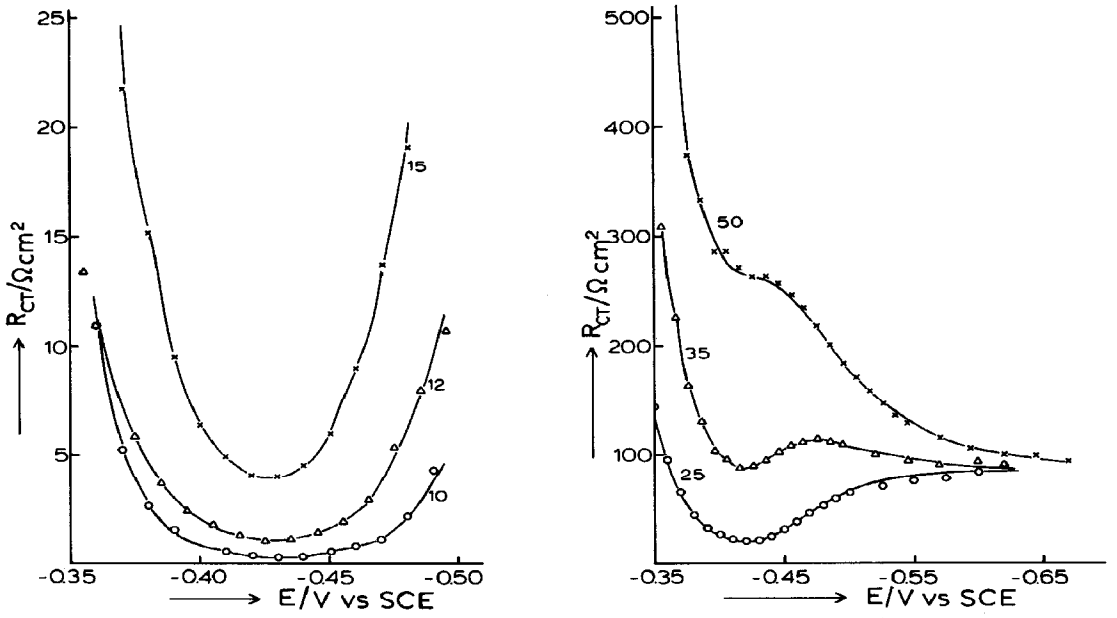

Fig. 3. The charge transfer resistance R_{ct} as a function of *dc* potential for the Sn(II) reduction from 1 M H_2SO_4 solution. (a) 1 mM $SnSO_4$ and (b) 3 mM $SnSO_4$. Concentrations of ENSA-6 are indicated in ppm.

considerably lower than its value in sulfuric acid and it could be obtained with the impedance technique from the charge transfer resistance at the relevant *dc* potentials.

The $\ln k_f$ *vs* potential relationship obtained, and also inserted in Fig. 4, is slightly curved. At positive potentials it tends to coincide with the straight line found in sulfuric acid, indicating the presence of the following chemical step C_3 in the mechanism.

At negative potentials the slope becomes close to $0.5(2F/RT)$, suggesting that the second, intermediate chemical step C_2 becomes rate determining. In the presence of 18 ppm ENSA-6 in the whole accessible potential region the slope is exactly $0.5(2F/RT)$.

The interpretation of this behaviour should be considered with some care. Instead of rate control by an intermediate chemical step, it is conceivable that the observed slope, $0.5(2F/RT)$, is due to the onset of rate control by the first electron transfer, or to a strong potential dependency of the adsorption of phenolsulphonic acid, which evidently has an influence on the reaction rate.

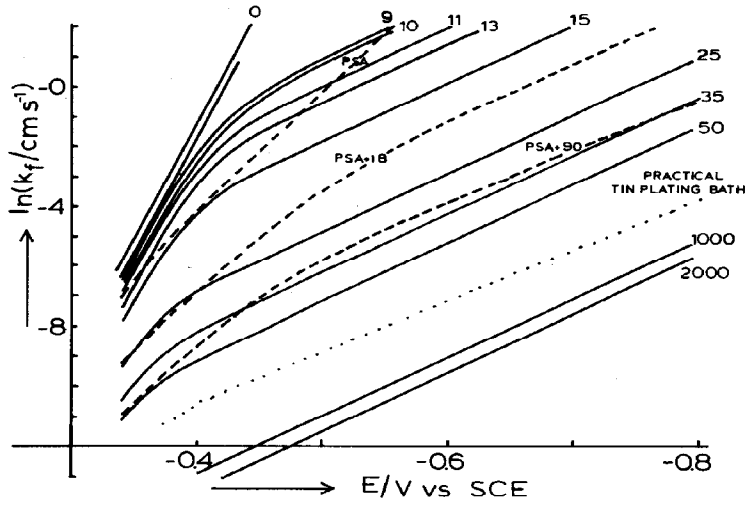

Fig. 4. Plots of $\ln k_f$ *vs* potential. (——) 1 M H_2SO_4 with ENSA-6 concentrations as indicated (in ppm); (– – –) phenolsulphonic acid with ENSA-6 concentrations as indicated; (. . .) the tin plating electrolyte.

Table 1

ENSA-6 (ppm)	k_{s1} (cm s^{-1})	k_c (cm s^{-1})	C_d at −500 mV (μF cm^{-2})	θ at −500 mV
0		3.5	30.2	0
1			29.0	0.048
5			22.6	0.306
7		2.2	18.8	0.460
10	0.57	1.7	15.5	0.593
11	0.27	1.2	13.3	0.680
13	0.16	0.79	12.0	0.733
15	0.043	0.51	10.8	0.782
25	0.0021	0.14	8.8	0.863
35	0.00051	0.05	8.4	0.880
50	0.00021	0.028	8.0	0.895
1000	4.6×10^{-6}		5.8	0.984
2000	2.8×10^{-6}		5.6	0.990

With a high concentration of inhibitor the slope becomes equal to the one found for the inhibited reaction in sulfuric acid, indicating control by the first electron transfer. In order to decelerate the reaction in phenolsulphonic acid to the same extent more than twice the amount of inhibitor is needed as compared with the sulfuric acid solution.

Reduction from a practical plating bath

Also in a practical tin plating bath containing 0.3 M phenolsulphonic acid, 0.25 M $SnSO_4$ and 2000 ppm ENSA-6 it was found that at the dropping mercury electrode the first electron transfer was rate determining. The $\ln k_f$ *vs* potential relationship found in this base electrolyte is reproduced in Fig. 4 as well. Also here the inhibitor appears to be less effective as compared with its behaviour in sulfuric acid, possibly because there is competition between the inhibitor and phenolsulphonic acid as for their adsorption.

The complex plane plots of the electrode impedance on varied *dc* potential and on varied frequency in the practical plating bath behave nicely according to the theoretical predictions[9 and refs cited therein] based on the Randles equivalent circuit. Some of these plots are reproduced in Fig. 5. Of course the application of such plots to obtain rate constants *via* the semicircle method is inferior to the numerical analysis developed later, but they are quite useful as a quick overview and for monitoring the quality of the bath in a practical situation.

DISCUSSION

From the results obtained it can be concluded that an inhibitor can slow down an electrode reaction in a rather complex way, having a different decelerating effect on the different steps in the mechanism.

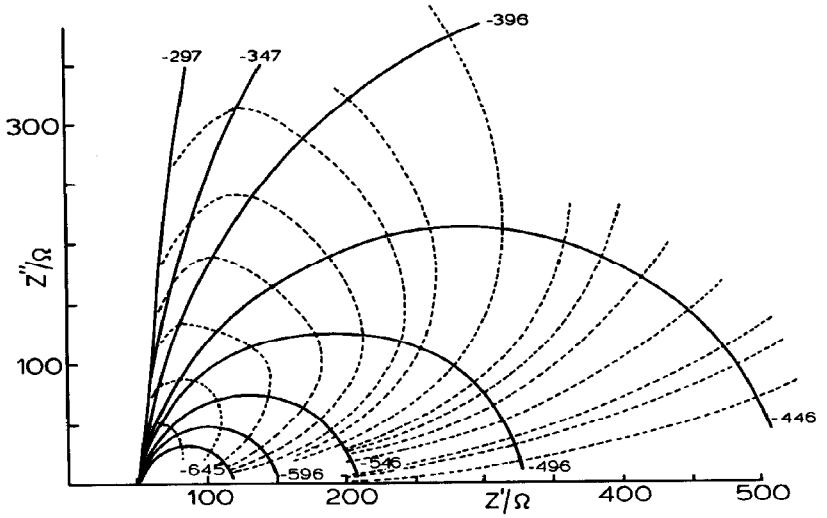

Fig. 5. Complex plane impedance plots of the *dme* in contact with the practical tin plating bath. (——) Plots at fixed potential and varied frequency (potentials indicated in mV *vs sce*); (– – –) plots at fixed frequency and varied potential.

As has been shown in the Theory the decelerating effect should not be studied as a function of the concentration of the inhibitor, but rather as a function of the amount adsorbed. A crude way to get an idea of the amount adsorbed is to determine a fractional coverage θ of the inhibitor from the double-layer data reported in Fig. 2, assuming that the value of the double-layer capacitance varies linearly with θ, so that θ can be calculated[10 and refs cited therein]:

$$\theta = \frac{C_d(\theta = 0) - C_d}{C_d(\theta = 0) - C_d(\theta = 1)}.$$

As all capacitances are potential dependent this should be done at all potentials to obtain θ as a function of potential. Here we shall confine to one potential, *viz.* -500 mV *vs sce*, and assume θ to be potential independent within the faradaic region.

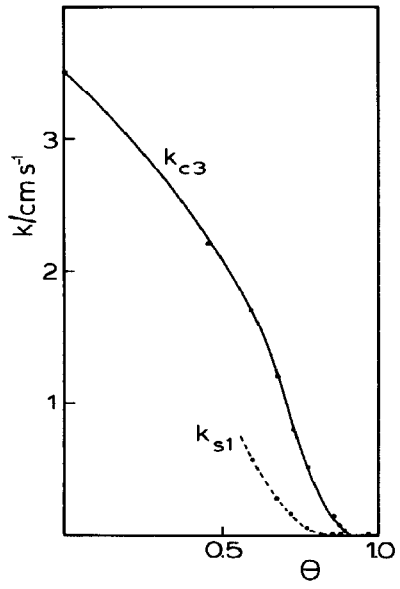

Fig. 6. The rate constants k_{c3} of the following chemical reaction step and k_{s1} of the first electron transfer step plotted against the fractional surface coverage θ.

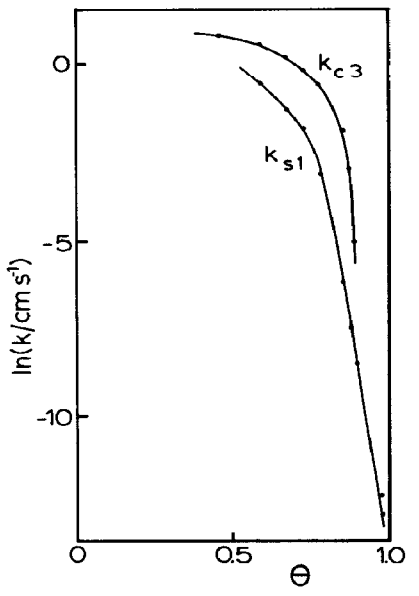

Fig. 7. The logarithm of the rate constants in Fig. 6 plotted against the fractional surface coverage θ.

Somewhat arbitrarily it has been assumed on the basis of these capacitance data, reported in Table 1, that maximum coverage corresponds to 5.4 μF cm^{-2}. The surface coverage θ calculated in this way is also reported in Table 1. Finally the rate constants k_{s1} and k_{c3} are visualized as a function of θ in Fig. 6.

Plotting the logarithm of k_{s1} and k_{c3} *vs* θ in Fig. 7 gives for k_{s1} a perfectly straight line for $\theta > 0.79$, which could mean that the inhibitor acts on the activation energy of the electron transfer at high surface coverage. The chemical step C_3, however, seems to be affected more linearly by the presence of the inhibitor, suggesting a mechanical blocking of this step up to $\theta = 0.9$.

It should be noted, however, that the ENSA-6 used in this work, consists of a mixture of naphtalene sulphonic acid ethoxylated with chains of different lengths. The surface coverage, determined as described above, might therefore be a less well-defined quantity. We intend to continue this work by a more detailed study of the adsorption behaviour of the inhibitor, as well as by a study of the effect of a better defined inhibitor on the reduction of tin.

Acknowledgements—This work is part of the chemistry research program (SON) of the Dutch Organization of Pure Scientific Research (ZWO) and was made possible by financial support from the Netherlands Technology Foundation (STW). The technical assistance of Mr J. M. Oostveen and valuable discussions with Mr E. Nagel Soepenberg and Dr H. Bunk, Hoogovens group, IJmuiden, The Netherlands are gratefully acknowledged.

REFERENCES

1. Kirk-Othmer, *Encyclopedia of Chemical Technology*, 3rd edn, Vol. 23, p. 28. Wiley, New York (1983).
2. B. N. Stirrup and N. A. Hampson, *Surf. Tech.* **5**, 429 (1977).
3. V. V. Gorodetskii, I. P. Slutskii and V. V. Losev, *Elektrokhimiya* **8**, 1401 (1972) (and refs cited therein).
4. J. Struijs, M. Sluyters-Rehbach and J. H. Sluyters, *J. electroanal. Chem.* **143**, 37, 61 (1983).
5. M. Sluyters-Rehbach and J. H. Sluyters, in *Electroanalytical Chemistry* (Edited by A. J. Bard), Vol. IV. Dekker, New York (1970).
6. C. P. M. Bongenaar, M. Sluyters-Rehbach and J. H. Sluyters, *J. electroanal. Chem.* **109**, 23 (1980).
7. C. P. M. Bongenaar, A. G. Remijnse, M. Sluyters-Rehbach and J. H. Sluyters, *J. electroanal. Chem.* **111**, 139 (1980).
8. J. Struijs, M. Sluyters-Rehbach and J. H. Sluyters, *J. electroanal. Chem.* **171**, 157, 177 (1984).
9. M. Sluyters-Rehbach and J. H. Sluyters, in *Comprehensive Treatise of Electrochemistry* (Edited by E. Yeager, J. O'MBockris, B. E. Conway and S. Sarangapani), Vol. 9, Chapter 4. A.C. Techniques (1984).
10. P. Delahay, *Double Layer and Electrode Kinetics*. Wiley, New York (1965).